

SUPPRESSORS OF SELECTION

FERNANDO ALCALDE CUESTA^{1,2}, PABLO GONZÁLEZ SEQUEIROS^{1,3},
AND ÁLVARO LOZANO ROJO^{1,4,5}

ABSTRACT. Inspired by recent works on evolutionary graph theory, an area of growing interest in mathematical and computational biology, we present the first known examples of undirected structures acting as suppressors of selection for any fitness value $r > 1$. This means that the average fixation probability of an advantageous mutant or invader individual placed at some node is strictly less than that of this individual placed in a well-mixed population. This leads the way to study more robust structures less prone to invasion, contrary to what happens with the amplifiers of selection where the fixation probability is increased on average for advantageous invader individuals. A few families of amplifiers are known, although some effort was required to prove it. Here, we use computer aided techniques to find an exact analytical expression of the fixation probability for some graphs of small order (equal to 6, 8 and 10) proving that selection is effectively reduced for $r > 1$. Some numerical experiments using Monte Carlo methods are also performed for larger graphs.

1. INTRODUCTION

Evolutionary dynamics has been classically studied for well-mixed populations, but there is a wide interest in the evolution of complex networks after site invasion. The process transforming nodes occupied by residents into nodes occupied by mutants or invaders is described by the *Moran model*. Introduced by Moran [1] as the Markov chain counting the number of invading mutants in a well-mixed population, it was adapted to weighted graphs by Lieberman et al. [2] and Nowak [3] (see also [4, 5, 6, 7, 8]). For undirected networks where links have no orientation, invaders will either become extinct or take over the whole population, reaching one of the two absorbing states, *extinction* or *fixation*. The *fixation probability* is the fundamental quantity in the stochastic evolutionary analysis of a finite population.

If the population is well-mixed, at the beginning, one single node is chosen to be occupied by an invader individual among a population of N resident individuals. Afterwards, an individual is randomly chosen for reproduction, with probability proportional to its reproductive advantage (1 for residents and $r \geq 1$ for invaders), and its clonal offspring replaces another individual chosen at random. In this case, the fixation probability is given by

$$(1) \quad \Phi_0(r) = \frac{1 - r^{-1}}{1 - r^{-N}} = \frac{r^{N-1}}{r^{N-1} + r^{N-2} + \dots + r + 1}.$$

Date: November 1, 2021.

Key words and phrases. Systems biology, evolutionary dynamics, Moran model, natural selection, fixation probability.

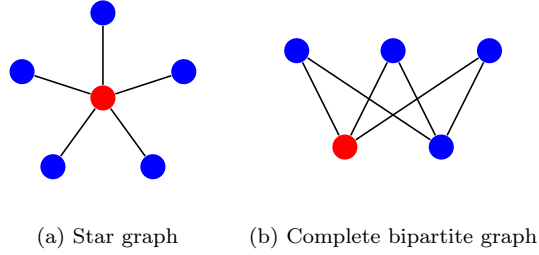


FIGURE 1. **Star and complete bipartite graphs.** (a) In the star graph $K_{1,m}$, the center is connected with m peripheral nodes. (b) The vertex set of a complete bipartite graph $K_{n,m}$ is divided into two disjoint sets interconnected by edges.

In evolutionary network theory, the nodes are occupied by resident or invader individuals and the replacements are limited to the nodes which are connected by oriented links. According to the Circulation Theorem [2], any weight-balanced network has the same fixation probability as the well-mixed population of the same size N . In the undirected case, this means that the temperature $T_i = \sum_{j \sim i} 1/d_j$ of every vertex i (where j is a neighbor of i and d_j is the number of neighbors of j) is constant, and the network is said to be *isothermal*. But there are graph structures altering substantially the behavior of the fixation probability depending on the fitness. For example, the (average) fixation probability in the oriented line is equal to $1/N$ and the reproductive advantage of the invader individuals is completely suppressed. But in the directed case, absorbing barriers may not be accessible from any state, and the fixation probability may be even null (see [9] for an example).

Thus, we focus our attention on undirected networks where absorbing barriers can be reached from any state. As showed in [2, 3] (see also [10]), there are directed and undirected graph structures that asymptotically amplify this advantage. The fixation probability of a complete bipartite network $K_{N-m,m}$ (described in Figure 1) converges to the same limit as the fixation probability

$$(2) \quad \Phi_2(r) = \Phi_0(r^2) = \frac{1 - r^{-2}}{1 - r^{-2N}}$$

of the Moran process with fitness r^2 as $m \rightarrow \infty$ and $N-m$ is constant [9]. Assuming that fitness differences are amplified or reduced for network sequences of increasing size, a notion of *amplifier* and *suppressor of selection* has been introduced in [10] for several initialization types (describing the initial distribution of the invasion process). To distinguish both dynamics, a numerical analysis for a few fitness values $r = 0.75, 1, 1.25, 1.5, 1.75$ has been done in [11] for birth-death and death-birth processes on directed and undirected graphs (see [12] for a comparative analysis of both update mechanisms).

Here we always assume that the distribution is uniform: the probability that a node will be occupied by the initial invader is equal for all the nodes (see Eq (5)). We say that a network is an *amplifier of selection* if the fixation probability function $\Phi(r) > \Phi_0(r)$ and a *suppressor of selection* if $\Phi(r) < \Phi_0(r)$ for all $r > 1$. Notice

that $\Phi(1) = 1/N$ and the inequalities must be reversed for $r < 1$. Due to the exact analytical expression given by Monk et al. [13] using martingales (see also [10]), one can see that star graphs and complete bipartite graph are amplifiers of natural selection whose fixation functions are bounded from above by $\Phi_2(r)$. One could also ask if the fixation function is always greater than or equal to that of a well-mixed population of the same size, denoted by $\Phi_0(r)$, at least from some fitness value. A negative answer to the first question was given in [14] for fitness values $r \leq 10$. The aim of the paper is to prove that both questions are not true, exhibiting examples of graphs with 6, 8 and 10 vertices which are suppressors of selection for any fitness value $r > 1$. From the point of view of robustness against invasion [15], these graphs are more robust than complete graphs (being now necessary to add a sign to $\|\Phi - \Phi_0\|_\infty = \sup_{r \geq 1} |\Phi(r) - \Phi_0(r)|$). Better yet, we propose a complete family of graphs of even order $2n + 2$ with $n \geq 2$, called ℓ -graphs, which we believe are suppressors of selection. The proof of this assertion for the graphs of order 6, 8 and 10 is completed with a numerical simulation for larger orders. Some other variants are also explored numerically in order to understand why they are suppressors of selection.

2. RESULTS

All the examples of so-called suppressors of selection given in [2, 3] are directed graphs. The abundance of amplifiers and suppressors of selection has been explored numerically by Hindersin et al. in [11] for this kind of graphs under birth-death and death-birth updating. Different types of initialization or placement of new invaders have been distinguished in [10] in order to classify different evolutionary dynamics on directed graphs. As explained, we focus our attention on undirected graphs under uniform initialization.

Firstly, working with the *FinisTerrae2* supercomputer (we used 1024 cores of Haskell 2680v3 CPUs for almost 3 days) installed at CESGA, we computed the fixation probability of all undirected graphs of order 10 or less for fitness values r varying from 0.25 to 10 with step size of 0.25 [16]. We found an unique suppressor of selection of order 6, namely the graph ℓ_6 , although there are other possible suppressors in orders varying from 7 to 10. We constructed the graphs ℓ_8 and ℓ_{10} (as well the whole ℓ -family) from this initial example. More precisely, we call ℓ -graph an undirected graph of even order $N = 2n + 2 \geq 6$ obtained from the complete graph K_{2n} by dividing its vertex set into two halves with $n \geq 2$ vertices and adding 2 extra vertices. Each of them is connected to one of the halves of K_{2n} and with the other extra vertex. Graphs ℓ_6 , ℓ_8 and ℓ_{10} of order 6, 8 and 10 are shown in Figure 2.

2.1. Graphs ℓ_6 , ℓ_8 and ℓ_{10} are suppressors of selection. Computer aided techniques has been used to find exact analytical expressions of the fixation function Φ for the first elements of this family with orders 6, 8 and 10 (see Figure 2). This computation proves that the graphs ℓ_6 , ℓ_8 and ℓ_{10} are suppressors of selection with fixation functions $\Phi(r) < \Phi_0(r)$ for all $r > 1$ and $\Phi(r) > \Phi_0(r)$ for all $r < 1$.

At first, to bound the fixation probability from above, one could try to stop the process on ℓ_{2n+2} at the time that some extra vertex is occupied by a mutant.

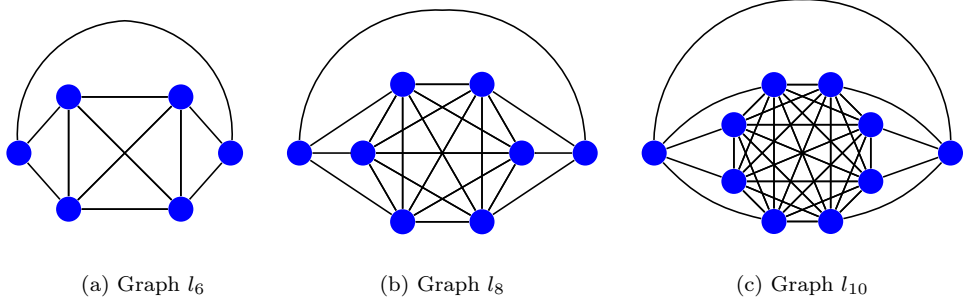


FIGURE 2. Graphs of size 6, 8 and 10 in the l -family.

But as we will see later, the evolution from that time on seems play an essential role in determining the suppressor character of the graph. Like for star and looping star graphs, which are amplifiers of selection for uniform initialization [10], we needed then to find the exact analytical expression of the fixation probability. Unfortunately, the elegant martingale method (which is based on Doob's optional stopping theorem [18]) proposed in [13] and used in [10] is not useful for ℓ_6 , ℓ_8 and ℓ_{10} . We have had to implement a specific method to compute exactly their fixation probability.

As we shall see in the description of the mathematical model in the Methods section, the fixation function $\Phi(r)$ is always a rational function given as the quotient of two rational polynomials $\Phi'(r)$ and $\Phi''(r)$ of degree bounded above by $2^N - 2$. Using the symmetries of each ℓ -graph, we can lower this bound to a quantity

$$(3) \quad d = \frac{N(N+1)}{2} - 2 \ll 2^N - 2$$

as proved in the Methods section, and hence there are and hence there are only $2(d+1)$ coefficients involved in $\Phi(r)$. Since $\Phi(r)$ converges to 1 as $r \rightarrow +\infty$, the leading coefficients of $\Phi'(r)$ and $\Phi''(r)$ can be assumed to be 1 and that number is reduced to $2d$. Then we can replace the system of 2^N linear equations defining the fixation function $\Phi(r)$ (see Eq (4)) with a system of $2d$ linear equations (see Eq (6)) corresponding to the $2d$ rational coefficients of $\Phi'(r)$ and $\Phi''(r)$, which arise from evaluating $\Phi(r)$ for integer and rational values of the fitness r varying from 1 to $d+1$ and from $1/2$ to $1/d$. Finally, we wrote a SageMath program [17] (which is added to the Supporting Information) to compute the exact fixation probability $\Phi(r)$ of the graphs ℓ_6 , ℓ_8 and ℓ_{10} for these fitness values and to solve the reduced linear system. Once the fixation function Φ has been calculated, the sign of the difference $\Delta = \Phi - \Phi_0$ is analyzed to confirm that $\Delta(r) < 0$ for all $r > 1$. In the Methods section, we give a more detailed explanation of both theoretical and computational arguments used to have exact analytical expressions of the fixation function Φ for ℓ_6 , ℓ_8 and ℓ_{10} . The exact values of Φ and Δ are given in the Supporting Information of the paper.

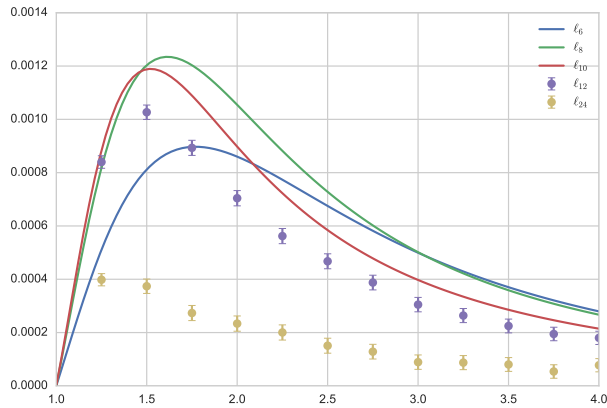


FIGURE 3. **The exact differences $\Phi_0(r) - \Phi(r)$ for ℓ_6 , ℓ_8 and ℓ_{10} and some estimates for ℓ_{12} and ℓ_{24} .** The functions $\Phi_0(r) - \Phi(r)$ associated to the ℓ -graphs of order 6, 8, and 10 are represented for fitness values r varying from 1 to 4. For the ℓ -graphs of order 12 and 24, we applied the Monte Carlo method to compute the difference between the fixation probabilities of each graph and the complete graph of the same order using 10^8 trials for each fitness value r varying from 0 to 4 with step size of 0.25. Notice that $\Phi_0(r) - \Phi(r)$ converges to 0 as the order of the graph goes to infinity for all fitness value $0 < r < +\infty$.

2.2. Numerical experiments in larger orders. Further examples. However, the method used for for ℓ_6 , ℓ_8 and ℓ_{10} does not seem to be applicable to larger orders since it would require a substantial amount of memory and computation time. Therefore, we explored the suppression of selection for other graphs in the ℓ -family using Monte Carlo simulation (applying the *Loop-Erasing* technique of [9] to speedup the computations). Even if it does not require much memory and can be parallelized on a computer cluster, a very large number of trials—namely 10^8 trails for each fitness value—has been necessary to compare the fixation probability of ℓ_{12} and ℓ_{24} with that of the complete graphs of the same order. In fact, since the fixation function of the ℓ -graph of order N approaches the fixation function $\Phi_0(r)$ given by Eq (1), we should need to increase this number more and more as N goes to ∞ . Anyway, for fitness values r varying from 0 to 4 with step size of 0.25, we showed that the ℓ -graphs of orders 12 and 24 are also suppressors of selection as can be seen in Figure 3.

To investigate the structural reasons of the suppression of selection in these graphs, this experiment has been completed by altering the balance in the connections of the two extra nodes with the central complete graph in order 6 and considering two variants (*a fortiori* unbalanced) of order 7 (see Figure 4). As showed in Figure 5, the graphs $\ell_6^{1,3}$ and $\ell_7^{1,4}$ become amplifiers of selection from relatively small values of the fitness, while the graph $\ell_7^{2,3}$ is a suppressor of selection for high fitness values. We discover a similar behaviour for larger orders (see Figure 6).

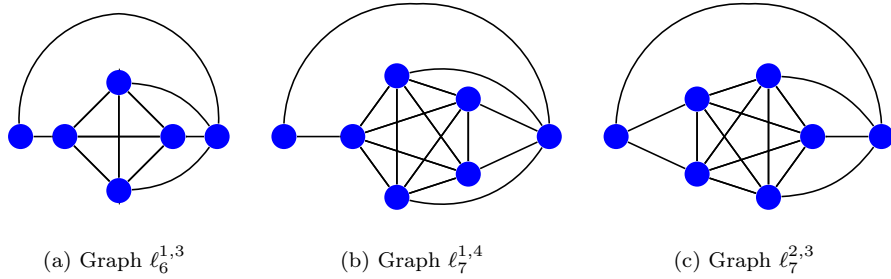


FIGURE 4. Unbalanced ℓ -graphs of order 6 and 7.

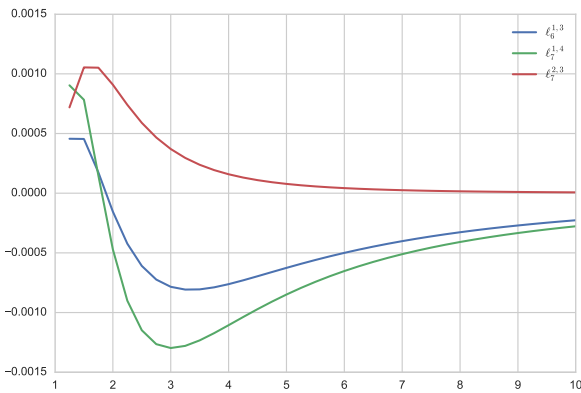


FIGURE 5. The differences $\Delta(r) = \Phi(r) - \Phi_0(r)$ for the unbalanced graphs $\ell_6^{1,3}$, $\ell_7^{1,4}$, and $\ell_7^{2,3}$. The differences $\Delta(r) = \Phi(r) - \Phi_0(r)$ have been estimated using 10^8 trials for each fitness value r varying from 0 to 10 with step size of 0.25.

3. DISCUSSION

Motivated by interest in the robustness of networks against invasion, we worked with the *FinisTerrae2* supercomputer (using 1024 cores of Haskell 2680v3 CPUs for almost 3 days) installed at CESGA to compute the fixation probability of all undirected graphs of order 10 or less for fitness values r varying from 0.25 to 10 with step size of 0.25 [16]. Exploring these data, it would be possible to shed some light on the influence of the structural properties of graphs upon increasing or decreasing the fixation probability of new invaders occupying the nodes of a network. In this paper, we proved that there are graph structures acting as suppressors of selection according to the terminology introduced in [2, 3]. This means that, for every fitness value $r > 1$, the average fixation probability $\Phi(r)$ of an advantageous invader individual placed at a random node is strictly less than that of this individual placed in a well-mixed population. For neutral drift $r = 1$, both probabilities $\Phi(1)$ and $\Phi_0(1)$ are obviously equal, whereas the average fixation probability $\Phi(r)$

becomes strictly greater than $\Phi_0(r)$ for a disadvantageous invader with fitness $r < 1$. We proposed a novel method to compute the fixation probability of graphs having low order and a big group of symmetries, and we used computer aided techniques to find an exact analytical expression of the fixation probability for three examples of size 6, 8 and 10. A SageMath program [17] to compute the fixation probability of these graphs is included in the Supporting Information of the paper. Monte Carlo simulation was also used to see with high precision that other graphs in this family are suppressors of selection for some fitness values (varying from 1 to 4 with step size of 0.25). Memory requirements make unfeasible to apply the same method for large orders, but it could be useful to study transitions between both regimes, suppression and amplification, in low order. On the other hand, although we are only concerned here with the evolutionary dynamics of graphs under birth-death updating, similarly to the work by Kaveh et al. [12] and Hindersin et al. [11], it could be also interesting to study the properties of the ℓ -family under death-birth updating. We also showed that the mechanism that activates the suppression of selection is quite subtle, since a certain imbalance in the number of nodes of the central complete graph which are connected with each additional node transforms our models into amplifiers from certain fitness values. Finally, if the spreading of favorable innovations can be enhanced by those network structures amplifying the advantage of mutant or invader individuals [19], as counterpart, the discovery of these examples is a first step towards finding structural properties that increase the robustness of a complex network against invasion [15]. This is a particularly interesting property for biological networks like brain networks or PPI interactomes, as well as for technological networks like electrical power grids or backbone networks, where high fitness values are possible. In fact, these kind of models have had impact not only in evolutionary and invasion dynamics, but also in tumor growth [3, 20, 21] and economics and management [22].

4. METHODS

4.1. Mathematical model. Let G be a connected undirected graph with node set $V = \{1, \dots, N\}$. Denote by d_i the degree of the node i . The *Moran process* on G is a Markov chain X_n whose states are the sets of nodes S inhabited by mutant or invader individuals at each time step n . The transition probabilities are obtained from a stochastic matrix $W = (w_{ij})$ where $w_{ij} = 1/d_i$ if $i \sim j$ and $w_{ij} = 0$ otherwise. More precisely, the transition probability between S and S' is given by

$$P_{S,S'} = \begin{cases} \frac{r \sum_{i \in S} w_{ij}}{w_G} & \text{if } S' \setminus S = \{j\}, \\ \frac{\sum_{i \in V \setminus S} w_{ij}}{w_G} & \text{if } S \setminus S' = \{j\}, \\ \frac{r \sum_{i,j \in S} w_{ij} + \sum_{i,j \in V \setminus S} w_{ij}}{w_G} & \text{if } S = S', \\ 0 & \text{otherwise,} \end{cases}$$

where $r > 0$ is the fitness and

$$w_G = r \sum_{i \in S} \sum_{j \in V} w_{ij} + \sum_{i \in V \setminus S} \sum_{j \in V} w_{ij} = r|S| + N - |S|$$

is the total reproductive weight of invaders and residents. The *fixation probability* of each subset $S \subset V$ inhabited by invaders $\Phi_S(r) = \mathbb{P}[\exists n \geq 0 : X_n = V \mid X_0 = S]$

gives a solution of the system of 2^N linear equations

$$(4) \quad \Phi_S(r) = \sum_{S'} P_{S,S'} \Phi_{S'}(r).$$

Since G is undirected, the only recurrent states are $S = \emptyset$ and $S = V$. Then Eq (4) has a unique solution [23]. The (*average*) *fixation probability* is given by

$$(5) \quad \Phi(r) = \frac{1}{N} \sum_{i=1}^N \Phi_{\{i\}}(r).$$

It is a rational function depending on the fitness $r \in (0, +\infty)$. Notice that $\Phi(r)$ may be calculated using the embedded Markov chain instead of the standard Markov chain above described, both associated to the process, making the total reproductive weight disappear from the computations [9].

4.2. Computation method. As we remarked above, the average fixation probability is a rational function $\Phi(r) = \Phi'(r)/\Phi''(r)$ where the numerator $\Phi'(r) = \sum_i a_i r^i$ and the denominator $\Phi''(r) = \sum_i b_i r^i$ are polynomials with rational coefficients of degree less than or equal to $2^N - 2$. Using the symmetries of each ℓ -graph, we can reduce the space of states $\mathcal{P}(V)$ to the set of 4-uplas

$$(e, k, k', e') \in \{0, 1\} \times \{0, 1, \dots, n\} \times \{0, 1, \dots, n\} \times \{0, 1\}$$

ordered lexicographically (from halves to extra vertices) by $k \geq k'$ or $e \geq e'$, or equivalently the system of linear equations Eq (4) to a new system with at most

$$\frac{(2(n+1))^2 + 2(n+1)}{2} = \frac{N^2 + N}{2} = \frac{N(N+1)}{2}$$

linear equations. For ℓ_6 , ℓ_8 and ℓ_{10} , we have 21, 36 and 55 reduced states respectively. Therefore, we can lower the former bound of the degree of $\Phi'(r)$ and $\Phi''(r)$ to a quantity

$$d = \frac{N(N+1)}{2} - 2$$

proving Eq (3). Hence, we should only compute the $2(d+1)$ coefficients involved in $\Phi(r)$. Actually, since $\Phi(r)$ converges to 1 as $r \rightarrow +\infty$, we can assume that $a_d = b_d = 1$. Thus, we can replace Eq (4) with the system of $2d$ linear equations

$$(6) \quad \sum_{i=0}^d a_i r^i = \Phi(r) \left(\sum_{i=0}^d b_i r^i \right),$$

which arise from evaluating the rational function $\Phi(r)$ for fitness values $r \in \{1, \dots, d+1, 1/2, \dots, 1/d\}$. This choice is due to those are the least complex rational numbers, which can be described with only few bits, and the length in bits of the solution of Eq (6) grows exponentially depending on the coefficients [24]. Finally, we wrote a SageMath program [17]

- to compute the exact fixation probability $\Phi(r)$ of the graphs ℓ_6 , ℓ_8 and ℓ_{10} for these fitness values,
- to solve the reduced linear system (6).

This program is included in the Supporting Information of the paper. Once the fixation function Φ of the graphs ℓ_6 , ℓ_8 and ℓ_{10} has been calculated solving this system, the sign of the numerator Δ' and the denominator Δ'' of the rational function $\Delta(r) = \Phi(r) - \Phi_0(r)$ is analyzed in order to prove that $\Delta(r) < 0$ for all $r > 1$. The exact values of Φ and Δ are also given in the Supporting Information.

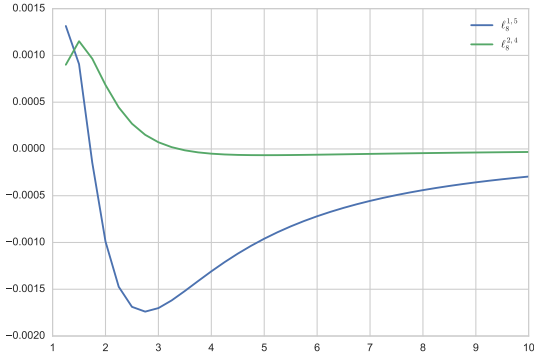
ACKNOWLEDGEMENTS

This work was supported by the Spanish Ministry of Economy and Competitiveness (Grant MTM2013-46337-C2-2-P), the Government of Galicia (Grant GPC2015/006) and the European Regional Development. Third author was also supported by the Government of Aragón and the European Regional Development Fund (Grant E15 Geometría) and the Defense University Center of Zaragoza (Grant CUD 2015-10). The authors thank the supercomputer facilities provided by CESGA.

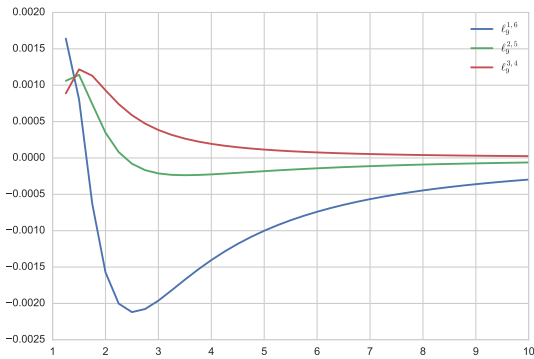
REFERENCES

- [1] P. A. P. Moran, "Random processes in genetics," *Proc. Cambridge Philos. Soc.*, vol. 54, pp. 60–71, 1958.
- [2] E. Lieberman, C. Hauert, and M. A. Nowak, "Evolutionary dynamics on graphs," *Nature*, vol. 433, no. 7023, pp. 312–316, Jan. 2005.
- [3] M. A. Nowak, *Evolutionary Dynamics: Exploring the Equations of Life*. Belknap Press of Harvard University Press, Sep. 2006.
- [4] M. Broom and J. Rychtář, "An analysis of the fixation probability of a mutant on special classes of non-directed graphs," *Proceedings of the Royal Society of London A: Mathematical, Physical and Engineering Sciences*, vol. 464, no. 2098, pp. 2609–2627, 2008. [Online]. Available: <http://rspa.royalsocietypublishing.org/content/464/2098/2609>
- [5] M. Broom, C. Hadjichrysanthou, J. Rychtář, and B. T. Stadler, "Two results on evolutionary processes on general non-directed graphs," *Proceedings of the Royal Society of London A: Mathematical, Physical and Engineering Sciences*, vol. 466, no. 2121, pp. 2795–2798, 2010. [Online]. Available: <http://rspa.royalsocietypublishing.org/content/466/2121/2795>
- [6] P. Shakarian, P. Roos, and A. Johnson, "A review of evolutionary graph theory with applications to game theory," *Biosystems*, vol. 107, no. 2, pp. 66 – 80, 2012.
- [7] P. Shakarian, P. Roos, and G. Moores, "A novel analytical method for evolutionary graph theory problems," *Biosystems*, vol. 111, no. 2, pp. 136 – 144, 2013. [Online]. Available: <http://www.sciencedirect.com/science/article/pii/S030326471300021X>
- [8] B. Voorhees and A. Murray, "Fixation probabilities for simple digraphs," *Proceedings of the Royal Society of London A: Mathematical, Physical and Engineering Sciences*, vol. 469, no. 2154, 2013. [Online]. Available: <http://rspa.royalsocietypublishing.org/content/469/2154/20120676>
- [9] F. Alcalde Cuesta, P. González Sequeiros, and Á. Lozano Rojo, "Fast and asymptotic computation of the fixation probability for moran processes on graphs," *Biosystems*, vol. 129, pp. 25 – 35, 2015. [Online]. Available: <http://www.sciencedirect.com/science/article/pii/S0303264715000088>
- [10] B. Adlam, K. Chatterjee, and M. A. Nowak, "Amplifiers of selection," *Proceedings of the Royal Society of London A: Mathematical, Physical and Engineering Sciences*, vol. 471, no. 2181, 2015. [Online]. Available: <http://rspa.royalsocietypublishing.org/content/471/2181/20150114>
- [11] L. Hindersin and A. Traulsen, "Most undirected random graphs are amplifiers of selection for birth-death dynamics, but suppressors of selection for death-birth dynamics," *PLoS Comput Biol*, vol. 11, no. 11, pp. 1–14, 11 2015. [Online]. Available: <http://dx.doi.org/10.1371%2Fjournal.pcbi.1004437>

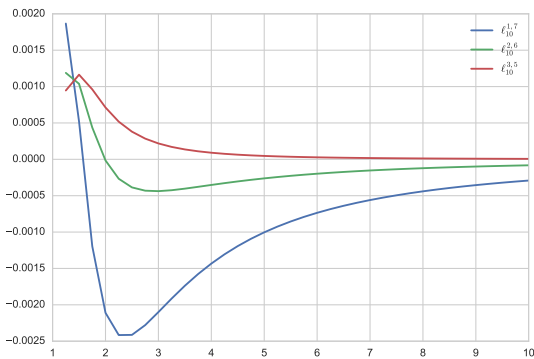
- [12] K. Kaveh, N. L. Komarova, and M. Kohandel, “The duality of spatial death–birth and birth–death processes and limitations of the isothermal theorem,” *Royal Society Open Science*, vol. 2, no. 4, 2015. [Online]. Available: <http://rsos.royalsocietypublishing.org/content/2/4/140465>
- [13] T. Monk, P. Green, and M. Paulin, “Martingales and fixation probabilities of evolutionary graphs,” *Proceedings of the Royal Society of London A: Mathematical, Physical and Engineering Sciences*, vol. 470, no. 2165, 2014. [Online]. Available: <http://rspa.royalsocietypublishing.org/content/470/2165/20130730>
- [14] M. Broom, J. Rychtář, and B. T. Stadler, “Evolutionary dynamics on graphs—the effect of graph structure and initial placement on mutant spread,” *J. Stat. Theory Pract.*, vol. 5, no. 3, pp. 369–381, 2011. [Online]. Available: <http://dx.doi.org/10.1080/15598608.2011.10412035>
- [15] F. Alcalde Cuesta, P. González Sequeiros, and Á. Lozano Rojo, “Exploring the topological sources of robustness against invasion in biological and technological networks,” *Scientific Reports*, vol. 6, pp. 20 666 EP –, 02 2016. [Online]. Available: <http://dx.doi.org/10.1038/srep20666>
- [16] F. Alcalde Cuesta, P. González Sequeiros, Á. Lozano Rojo, and R. Vigara, “An accurate database of the fixation probabilities of all undirected graphs of order 10 or less,” Submitted for publication, 2016.
- [17] W. A. Stein *et al.*, *Sage Mathematics Software (Version 5.8)*, The Sage Development Team, 2013, <http://www.sagemath.org>.
- [18] S. Karlin and H. M. Taylor, *A first course in stochastic processes*, 2nd ed. Academic Press [A subsidiary of Harcourt Brace Jovanovich Publishers], New York-London, 1975.
- [19] S. Tan and J. Lu, “Characterizing the effect of population heterogeneity on evolutionary dynamics on complex networks,” *Sci. Rep.*, vol. 4, p. 2014/05/22/online, 2014.
- [20] L. Hindersin, B. Werner, D. Dingli, and A. Traulsen, “Should tissue structure suppress or amplify selection to minimize cancer risk?” *Biology Direct*, vol. 11, no. 1, p. 41, 2016. [Online]. Available: <http://dx.doi.org/10.1186/s13062-016-0140-7>
- [21] N. L. Komarova, A. Sengupta, and M. A. Nowak, “Mutation-selection networks of cancer initiation: tumor suppressor genes and chromosomal instability,” *Journal of Theoretical Biology*, vol. 223, no. 4, pp. 433 – 450, 2003. [Online]. Available: <http://www.sciencedirect.com/science/article/pii/S0022519303001206>
- [22] V. Salas-Fumás, C. Sáenz-Royo, and A. Lozano-Rojo, “Organisational structure and performance of consensus decisions through mutual influences: A computer simulation approach,” *Decision Support Systems*, vol. 86, pp. 61 – 72, 2016. [Online]. Available: <http://www.sciencedirect.com/science/article/pii/S0167923616300422>
- [23] H. M. Taylor and S. Karlin, *An introduction to stochastic modeling*, 3rd ed. San Diego, CA: Academic Press Inc., 1998.
- [24] X. G. Fang and G. Havas, “On the worst-case complexity of integer gaussian elimination,” in *Proceedings of the 1997 International Symposium on Symbolic and Algebraic Computation*, ser. ISSAC ’97. New York, NY, USA: ACM, 1997, pp. 28–31. [Online]. Available: <http://doi.acm.org/10.1145/258726.258740>



(a) Unbalanced ℓ -graphs of order 8



(b) Unbalanced ℓ -graphs of order 9



(c) Unbalanced ℓ -graphs of order 10

FIGURE 6. The differences $\Delta(r) = \Phi(r) - \Phi_0(r)$ for the unbalanced graphs of order 8, 9, and 10.

Supporting Information

As supplementary information, we include here the text of the SageMath program which we ran

- to compute the exact fixation probability $\Phi(r)$ for the graphs ℓ_6 , ℓ_8 and ℓ_{10} when the fitness values $r \in \{1, \dots, d+1, 1/2, \dots, 1/d\}$,
- to solve the linear system

$$\sum_{i=0}^d a_i r^i = \Phi(r) \left(\sum_{i=0}^d b_i r^i \right),$$

where $\Phi'(r) = \sum_{i=0}^d a_i r^i$ and $\Phi''(r) = \sum_{i=0}^d b_i r^i$ are the numerator and the denominator of the rational function $\Phi(r)$. The symmetries of the graph allow to reduce the degree which is now bounded by $d = \frac{N(N+1)}{2} - 2 \ll 2^N - 2$. Next, we give the exact values of $\Phi = \Phi'/\Phi''$ and $\Delta = \Delta'/\Delta''$ for the graphs ℓ_6 , ℓ_8 and ℓ_{10} .

TEXT OF THE SAGEMATH PROGRAM

```

#
# The l-family checker
#
# The graph l_{2n+2} is a complete graph K_{2n} with two more nodes
# each of them connected with half the nodes of the complete core.
# These new nodes are also joint by an edge.
#
# The nodes are written as
#
#      (e,k,k',e')
#
# where e,e' \in \{0,1\} represents if the external nodes are mutants or not,
# and k,k' \in \{0,1,\dots,n\} the number of mutants of each halves of the complete
# core. Using the symmetries of the graph, it is possible to reduce the nodes
# to those with (lexicographically)
#
#      k >= k'           e >= e'
#
# The parameter n is:
n = 2 # change it to 3 and 4 to reproduce the results of the paper

#
# Reduces the state s to a canonical form
#
def reduce_state(s):
    if s[1] < s[2]:
        return (s[3],s[2],s[1],s[0])
    if (s[1] == s[2]) and (s[3] > s[0]):
        return (s[3],s[2],s[1],s[0])
    return s

```

```

#
# Computes the possible (reduced) states for a given n, it returns the list of
# states and the position of the states in the list
#
def ComputeStates(n):
    # Compute the states
    states = []
    for k in [0..n]:
        for kp in [0..k]:
            if k != kp:
                states.extend([(0,k,kp,0), (1,k,kp,0), (0,k,kp,1), (1,k,kp,1)])
            else:
                states.extend([(1,k,kp,1), (1,k,kp,0), (0,k,kp,0)])
    istates = { v:k for k,v in enumerate(states) }

    s0 = states[0]
    sn = states[-1]
    states[0] = (0,0,0,0)
    states[-1] = (1,n,n,1)
    states[istates[(0,0,0,0)]] = s0
    states[istates[(1,n,n,1)]] = sn
    istates[s0] = istates[(0,0,0,0)]
    istates[sn] = istates[(1,n,n,1)]
    istates[(0,0,0,0)] = 0
    istates[(1,n,n,1)] = len(states)-1
    return states, istates

#
# Computes the matrix P and the vector b for the list
#
def ComputePb(r,n,states,istates):

    # Compute matrix
    P = matrix(PP,[[0]*len(states)]*len(states) )

    for s in states:
        m = sum(s)
        P[istates[s],istates[s]] = r * m + 2 * n + 2 - m

    for s in states:
        # Leftmost
        if s[0] == 1:
            P[istates[s],istates[(1,s[1],s[2],1)]] -= r/(n+1)

```

```

if s[1] == n:
    P[istates[s],istates[s]] -= r*n/(n+1)
else:
    P[istates[s],istates[(s[0],s[1]+1,s[2],s[3])]] -= r*(n-s[1])/(n+1)
    P[istates[s],istates[s]] -= r*s[1]/(n+1)
else:
    P[istates[s],istates[(0,s[1],s[2],0)]] -= 1/(n+1)

if s[1] == 0:
    P[istates[s],istates[s]] -= n/(n+1)
else:
    P[istates[s],istates[reduce_state((s[0],s[1]-1,s[2],s[3]))]] -= s[1]/(n+1)
    P[istates[s],istates[s]] -= (n-s[1])/(n+1)

# Rightmost
if s[3] == 1:
    P[istates[s],istates[(1,s[1],s[2],1)]] -= r/(n+1)
    if s[2] == n:
        P[istates[s],istates[s]] -= r*n/(n+1)
    else:
        P[istates[s],istates[reduce_state((s[0],s[1],s[2]+1,s[3]))]] -= r*(n-s[2])/(n+1)
        P[istates[s],istates[s]] -= r*s[2]/(n+1)
else:
    P[istates[s], istates[(0,s[1],s[2],0)]] -= 1/(n+1)

if s[2] == 0:
    P[istates[s],istates[s]] -= n/(n+1)
else:
    P[istates[s],istates[(s[0],s[1],s[2]-1,s[3])]] -= s[2]/(n+1)
    P[istates[s],istates[s]] -= (n-s[2])/(n+1)

# Core left
if s[1] == n:
    P[istates[s],istates[(1,n,s[2],s[3])]] -= r/2
    P[istates[s],istates[s]] -= r*(n-1)/2
    if s[2] == n:
        P[istates[s],istates[s]] -= r*n/2
    else:
        P[istates[s],istates[reduce_state((s[0],n,s[2]+1,s[3]))]] -= r*(n-s[2])/2
        P[istates[s],istates[s]] -= r*s[2]/2
elif s[1] == 0:
    P[istates[s],istates[(s[3],0,0,0)]] -= 1/2
    P[istates[s],istates[s]] -= (n-1)/2 + n/2
else:
    P[istates[s],istates[(1,s[1],s[2],s[3])]] -= s[1]*r/(2*n)
    P[istates[s],istates[reduce_state((0,s[1],s[2],s[3]))]] -= (n-s[1])/(2*n)
    P[istates[s],istates[s]] -= s[1]*r*(s[1]-1)/(2*n) + (n-s[1])*(n-s[1]-1)/(2*n)

```

```

P[istates[s],istates[(s[0],s[1]+1,s[2],s[3])]] -= s[1]*r*(n-s[1])/(2*n)
P[istates[s],istates[reduce_state((s[0],s[1]-1,s[2],s[3]))]] -= (n-s[1])*s[1]/(2*n)
P[istates[s],istates[s]] -= r*s[1]*s[2]/(2*n) + (n-s[1])*(n-s[2])/(2*n)
P[istates[s],istates[reduce_state((s[0],s[1],s[2]+1,s[3]))]] -= r*s[1]*(n-s[2])/(2*n)

if s[2] != 0:
    P[istates[s],istates[(s[0],s[1],s[2]-1,s[3])]] -= (n-s[1])*s[2]/(2*n)

# Core right
if s[2] == n:
    P[istates[s],istates[(1,n,n,s[0])]] -= r/2
    P[istates[s],istates[s]] -= r*(2*n-1)/2
elif s[2] == 0:
    P[istates[s],istates[(s[0],s[1],0,0)]] -= 1/2

if s[1] == 0:
    P[istates[s],istates[s]] -= (2*n-1)/2
else:
    P[istates[s],istates[s]] -= (n-1)/2 + (n-s[1])/2
    P[istates[s],istates[reduce_state((s[0],s[1]-1,0,s[3]))]] -= s[1]/2
else:
    P[istates[s],istates[reduce_state((s[0],s[1],s[2],1))]] -= s[2]*r/(2*n)
    P[istates[s],istates[(s[0],s[1],s[2],0)]] -= (n-s[2])/(2*n)
    P[istates[s],istates[s]] -= s[2]*r*(s[2]-1)/(2*n) + (n-s[2])*(n-s[2]-1)/(2*n)
    P[istates[s],istates[s]] -= r*s[2]*s[1]/(2*n) + (n-s[2])*(n-s[1])/(2*n)
    P[istates[s],istates[reduce_state((s[0],s[1],s[2]+1,s[3]))]] -= s[2]*r*(n-s[2])/(2*n)
    P[istates[s],istates[(s[0],s[1],s[2]-1,s[3])]] -= (n-s[2])*s[2]/(2*n)
    if s[1] != n:
        P[istates[s],istates[(s[0],s[1]+1,s[2],s[3])]] -= r*s[2]*(n-s[1])/(2*n)
        P[istates[s],istates[reduce_state((s[0],s[1]-1,s[2],s[3]))]] -= (n-s[2])*s[1]/(2*n)

b=-P[1:len(states)-1,len(states)-1]
P=P[1:len(states)-1,1:len(states)-1]
return P,b

#
# Computes the average fixation probability function
#
def Phi(P,b,n,istates):
    sol = P.solve_right(b)
    return sol[istates[(1,0,0,0)]-1,0] / (n + 1) + sol[istates[(0,1,0,0)]-1,0] * n / (n + 1)

#
# "Entry point"
#

```

```

# Computes the states for the given size
states, istates = ComputeStates(n)

# A first estimate of the degree of the rational function Phi
num_fac = len(states) - 2
fits=[1..num_fac+1]
fits.extend([ 1/f for f in fits[1:-1] ])

# Compute the fixation probabilities for the selected fitnesses
fps = {
    f : Phi(*ComputePb(f, n, states, istates), n=n, istates=istates)
        for f in fits
}

# Now we are ready to compute the coefficients of the function.
# Construct the matrix of the linear system describing the function \Phi
X = matrix(PP, [[1]*len(fits)]*len(fits) )
X[:,num_fac-2] = [ [r] for r in fits ]
X[:, -1] = [ [-fps[r]] for r in fits ]
X[:, -2] = [ [-r*fps[r]] for r in fits ]

y = vector(PP, [(fps[r]-1)*r**num_fac for r in fits] )

for i in xrange(num_fac-3,-1,-1):
    X[:,i] = X[:,i+1].elementwise_product( X[:,num_fac-2] )
    X[:,num_fac + i] = X[:,num_fac+i+1].elementwise_product( X[:,num_fac-2] )

# Solve it
sol = X.solve_right(y)

# Create the field of functions. Then x is regarded as the variable of the
# field P(x). You can bypass this step to simplify later the expressions
# (that is regarding x as a symbolic variable with no special meaning)
F.<x> = Frac(PP['x'])

# Construct the function
FB = (sum( sol[num_fac-1-i]*x**i for i in [0..num_fac-1] ) + x**num_fac) / \
      (sum( sol[-(i+1)]*x**i for i in [0..num_fac-1] ) + x**num_fac)
pretty_print(FB)

# and finally the Delta
Delta = FB - x**(2*n+1)/sum( x**i for i in range(2*n+2) )
pretty_print(Delta)

# take a look to the numerator and denominator
pretty_print(Delta.denominator())
pretty_print(Delta.numerator()/(x-1)) # up to (x-1)

```

FIXATIONS FUNCTIONS FOR ℓ_6 , ℓ_8 AND ℓ_{10}

Graph ℓ_6

$$\begin{aligned} \Phi'(r) &= r^{17} + \frac{20010803101}{2356885440}r^{16} + \frac{12872954057}{368903808}r^{15} + \frac{146529682470259}{1590897672000}r^{14} + \frac{20006411662050293}{114544632384000}r^{13} + \\ &\quad \frac{57705463723529081}{229089264768000}r^{12} + \frac{9771555843017869}{34363389715200}r^{11} + \frac{1025122250624863}{4042751731200}r^{10} + \frac{60836752923313811}{343633897152000}r^9 + \\ &\quad \frac{9233243223215201}{98181113472000}r^8 + \frac{154239240426107}{42954237144000}r^7 + \frac{3153322564729}{357951976200}r^6 + \frac{496442293}{474304896}r^5 \\ \Phi''(r) &= r^{17} + \frac{22367688541}{2356885440}r^{16} + \frac{1883112090533}{42423937920}r^{15} + \frac{579196292648299}{76363088256000}r^{14} + \frac{23779172425823219}{42423937920}r^{13} + \\ &\quad \frac{17230349794290811}{37885437915832519}r^{12} + \frac{5592085032472109}{65454075648000}r^{11} + \frac{71798191286820983}{65454075648000}r^{10} + \frac{37885437915832519}{30545235302400}r^9 + \\ &\quad \frac{37885437915832519}{30545235302400}r^8 + \frac{71798191286820983}{65454075648000}r^7 + \frac{5592085032472109}{65454075648000}r^6 + \frac{17230349794290811}{30545235302400}r^5 + \\ &\quad \frac{30545235302400}{23779172425823219}r^4 + \frac{65454075648000}{579196292648299}r^3 + \frac{1883112090533}{42423937920}r^2 + \frac{23367688541}{2356885440}r + 1 \\ \Delta'(r) &= r^5(r-1)\left(-\frac{1}{408}r^{13} - \frac{17959403797}{509087255040}r^{12} - \frac{2269495014623}{9163570590720}r^{11} - \frac{16593379973713}{152726176512000}r^{10} - \right. \\ &\quad \left.\frac{4365681088426001}{137453558608000}r^9 - \frac{448781187686051}{13704670736178649}r^8 - \frac{687267794304000}{137453558608000}r^7 - \frac{673669214287879}{59762416896000}r^6 - \right. \\ &\quad \left.\frac{137453558608000}{299174081287}r^5 - \frac{2361661570426121}{299174081287}r^4 - \frac{2506212053017441}{687267794304000}r^3 - \frac{122207986609099}{85908474288000}r^2 - \right. \\ &\quad \left.\frac{137453558608000}{818175945600}r^1 - \frac{22137397}{474304896}\right) \\ \Delta''(r) &= r^{21} + \frac{22367688541}{2356885440}r^{20} + \frac{1925536028453}{42423937920}r^{19} + \frac{619458132022099}{42423937920}r^{18} + \frac{27245137277038619}{76363088256000}r^{17} + \\ &\quad \frac{15493177389178517}{1329324154659596831}r^{16} + \frac{552157240360000477}{458178529536000}r^{15} + \frac{411797892764062669}{229089264768000}r^{14} + \frac{550050599259865931}{229089264768000}r^{13} + \\ &\quad \frac{1308203195769664571995777599649}{500050599259865931}r^{24} + \frac{92197306752696283843238979311641}{55215740360000477}r^{23} + \\ &\quad \frac{25100123467406200012800000}{11740712284825831069430912101427861}r^{22} + \frac{12437849170258405340160000}{1032937952392948232127781620508111}r^{21} + \\ &\quad \frac{101806100783799547251916800000}{2080310449462551016365104268144504161}r^{20} + \frac{6568135534438680467865600000}{753897025982731385467385013243433}r^{19} + \\ &\quad \frac{1099505884650351103207104400000}{24635466779770270651137435076943581}r^{18} + \frac{3739815947159983368437760000}{1251563161394232439985295422113577}r^{17} + \\ &\quad \frac{129353633937062954155376640000}{347790118541691168774411224802753}r^{16} + \frac{551043772088520077122578161372417}{7853613489035965073719296000}r^{15} + \\ &\quad \frac{29556609904974062105395200000}{470903112909175542318799571869746773}r^{14} + \frac{596923826377497575290462451325719}{28934365485921976587386880000}r^{13} + \\ &\quad \frac{1099505884650351103207014400000}{7066876349108602065069037131219649}r^{12} + \frac{152306586352580143385602731564041827}{54975739442325175551603507200000}r^{11} + \\ &\quad \frac{141930027424171970518414844712131}{6249152838837548879426501}r^{10} + \frac{911745036811073646792134165773}{6544677907529970894766080000}r^9 + \\ &\quad \frac{196340337225899126842982400000}{354149237420452970496000}r^8 + \frac{11363885694605603}{10303182674104320}r^7 \\ \Phi''(r) &= r^{31} + \frac{142590263789341}{8309364148800}r^{30} + \frac{51436353602527862867}{399248328621542400}r^{29} + \\ &\quad \frac{261395239481852545538087881}{387350728428620436480000}r^{28} + \frac{58380787959652779590779931453}{22369504566752830206720000}r^{27} + \\ &\quad \frac{273244285509514020032806460287}{109546794936308370917902477449001}r^{25} + \\ &\quad \frac{3441462241038896954880000}{1038203195769664571995777599649}r^{24} + \frac{554186435718263644761600000}{92197306752696283843238979311641}r^{23} + \\ &\quad \frac{25100123467406200012800000}{11740712284825831069430912101427861}r^{22} + \frac{12437849170258405340160000}{1032937952392948232127781620508111}r^{21} + \\ &\quad \frac{101806100783799547251916800000}{2080310449462551016365104268144504161}r^{20} + \frac{6568135534438680467865600000}{753897025982731385467385013243433}r^{19} + \\ &\quad \frac{1099505884650351103207104400000}{24635466779770270651137435076943581}r^{18} + \frac{3739815947159983368437760000}{1251563161394232439985295422113577}r^{17} + \\ &\quad \frac{129353633937062954155376640000}{347790118541691168774411224802753}r^{16} + \frac{551043772088520077122578161372417}{7853613489035965073719296000}r^{15} + \\ &\quad \frac{29556609904974062105395200000}{470903112909175542318799571869746773}r^{14} + \frac{596923826377497575290462451325719}{28934365485921976587386880000}r^{13} + \\ &\quad \frac{1099505884650351103207014400000}{7066876349108602065069037131219649}r^{12} + \frac{152306586352580143385602731564041827}{54975739442325175551603507200000}r^{11} + \\ &\quad \frac{141930027424171970518414844712131}{6249152838837548879426501}r^{10} + \frac{911745036811073646792134165773}{6544677907529970894766080000}r^9 + \\ &\quad \frac{196340337225899126842982400000}{354149237420452970496000}r^8 + \frac{11363885694605603}{10303182674104320}r^7 \\ \Phi''(r) &= r^{31} + \frac{142590263789341}{8309364148800}r^{30} + \frac{685751104869983351}{4697039160253440}r^{29} + \\ &\quad \frac{317970272348671658716148800}{387350728428620436480000}r^{28} + \frac{614045446315686238195542724177}{1789560363534022641653760000}r^{27} + \\ &\quad \frac{782883035835001850913227050807}{2027468204090641240495620587659}r^{25} + \\ &\quad \frac{68829244820777939097600000}{65074922376008233328640000}r^{24} + \\ &\quad \frac{6233679485365536931871855089022867}{54059973838853275954244381013403073}r^{23} + \\ &\quad \frac{8589889753633086799380400000}{36813813229856086283059200000}r^{22} + \\ &\quad \frac{54122335023003970350539078924384011}{173354579809818706001364139420724667}r^{21} + \\ &\quad \frac{206157354087194083185131520000}{4123147081743881663702630400000}r^{20} + \\ &\quad \frac{167761731499454621427769594600403}{133786488706719539236595661589558203}r^{19} + \\ &\quad \frac{2748764721162587775801753600000}{1649258832697552665481052160000}r^{18} + \\ &\quad \frac{107094729395447827740615186917132468293}{937459378090858152054746159000953163}r^{17} + \\ &\quad \frac{39696361687927740615186917132468293}{8246294163487763327405260800000}r^{16} + \\ &\quad \frac{32723389537649854473830400000}{32723389537649854473830400000}r^{15} + \\ &\quad \frac{9374593978090858152054746159000953163}{10664177881341717213997454149404519}r^{14} + \\ &\quad \frac{8246294163487763327405260800000}{1070947293954478277990400000}r^{13} + \\ &\quad \frac{1337864897706719539236595661589558203}{167761731499454621427769594600403}r^{12} + \\ &\quad \frac{1649258832697552665481052160000}{2748764721162587775801753600000}r^{11} + \\ &\quad \frac{173354579809817100601364139420724667}{54122335023003970350539078924384011}r^{10} + \\ &\quad \frac{4123147081743881663702630400000}{206157354087194083185131520000}r^9 + \\ &\quad \frac{5405997383885275954244381013403073}{6233679485365536931871855089022867}r^8 + \\ &\quad \frac{36813813229856086283059200000}{85898897536330867993804800000}r^7 + \\ &\quad \frac{2027468204090641240495620587659}{68829244820777939097600000}r^6 + \frac{782883035835001850913227050807}{68829244820777939097600000}r^5 + \end{aligned}$$

Graph ℓ_8

$$\begin{aligned} \Phi'(r) &= r^{31} + \frac{134280899640541}{8309364148800}r^{30} + \frac{51436353602527862867}{399248328621542400}r^{29} + \\ &\quad \frac{261395239481852545538087881}{387350728428620436480000}r^{28} + \frac{58380787959652779590779931453}{22369504566752830206720000}r^{27} + \\ &\quad \frac{273244285509514020032806460287}{109546794936308370917902477449001}r^{25} + \\ &\quad \frac{3441462241038896954880000}{103820319576966457199577599649}r^{24} + \frac{554186435718263644761600000}{92197306752696283843238979311641}r^{23} + \\ &\quad \frac{25100123467406200012800000}{11740712284825831069430912101427861}r^{22} + \frac{12437849170258405340160000}{1032937952392948232127781620508111}r^{21} + \\ &\quad \frac{101806100783799547251916800000}{2080310449462551016365104268144504161}r^{20} + \frac{6568135534438680467865600000}{753897025982731385467385013243433}r^{19} + \\ &\quad \frac{1099505884650351103207014400000}{24635466779770270651137435076943581}r^{18} + \frac{3739815947159983368437760000}{1251563161394232439985295422113577}r^{17} + \\ &\quad \frac{129353633937062954155376640000}{347790118541691168774411224802753}r^{16} + \frac{551043772088520077122578161372417}{7853613489035965073719296000}r^{15} + \\ &\quad \frac{29556609904974062105395200000}{470903112909175542318799571869746773}r^{14} + \frac{596923826377497575290462451325719}{28934365485921976587386880000}r^{13} + \\ &\quad \frac{1099505884650351103207014400000}{7066876349108602065069037131219649}r^{12} + \frac{152306586352580143385602731564041827}{54975739442325175551603507200000}r^{11} + \\ &\quad \frac{141930027424171970518414844712131}{6249152838837548879426501}r^{10} + \frac{911745036811073646792134165773}{6544677907529970894766080000}r^9 + \\ &\quad \frac{196340337225899126842982400000}{354149237420452970496000}r^8 + \frac{11363885694605603}{10303182674104320}r^7 \\ \Phi''(r) &= r^{31} + \frac{142590263789341}{8309364148800}r^{30} + \frac{685751104869983351}{4697039160253440}r^{29} + \\ &\quad \frac{317970272348671658716148800}{387350728428620436480000}r^{28} + \frac{614045446315686238195542724177}{1789560363534022641653760000}r^{27} + \\ &\quad \frac{782883035835001850913227050807}{2027468204090641240495620587659}r^{25} + \\ &\quad \frac{68829244820777939097600000}{65074922376008233328640000}r^{24} + \\ &\quad \frac{6233679485365536931871855089022867}{54059973838853275954244381013403073}r^{23} + \\ &\quad \frac{8589889753633086799380400000}{36813813229856086283059200000}r^{22} + \\ &\quad \frac{54122335023003970350539078924384011}{206157354087194083185131520000}r^{21} + \\ &\quad \frac{206157354087194083185131520000}{4123147081743881663702630400000}r^{20} + \\ &\quad \frac{167761731499454621427769594600403}{1337864897706719539236595661589558203}r^{19} + \\ &\quad \frac{2748764721162587775801753600000}{1649258832697552665481052160000}r^{18} + \\ &\quad \frac{1070947293954478277990400000}{937459378090858152054746159000953163}r^{17} + \\ &\quad \frac{1337864897706719539236595661589558203}{167761731499454621427769594600403}r^{16} + \\ &\quad \frac{2748764721162587775801753600000}{1649258832697552665481052160000}r^{15} + \\ &\quad \frac{1070947293954478277990400000}{937459378090858152054746159000953163}r^{14} + \\ &\quad \frac{10664177881341717213997454149404519}{1337864897706719539236595661589558203}r^{13} + \\ &\quad \frac{8246294163487763327405260800000}{1070947293954478277990400000}r^{12} + \\ &\quad \frac{1649258832697552665481052160000}{2748764721162587775801753600000}r^{11} + \\ &\quad \frac{173354579809817100601364139420724667}{54122335023003970350539078924384011}r^{10} + \\ &\quad \frac{4123147081743881663702630400000}{206157354087194083185131520000}r^9 + \\ &\quad \frac{5405997383885275954244381013403073}{6233679485365536931871855089022867}r^8 + \\ &\quad \frac{36813813229856086283059200000}{85898897536330867993804800000}r^7 + \\ &\quad \frac{2027468204090641240495620587659}{68829244820777939097600000}r^6 + \frac{782883035835001850913227050807}{68829244820777939097600000}r^5 + \end{aligned}$$

$$\begin{aligned}
& \frac{614045446315686238195542724177}{178956036534022641653760000} r^4 + \frac{317970272348671658719761481}{387350728428620436480000} r^3 + \\
& \frac{685751104869983351}{4697039160253440} r^2 + \frac{142590263789341}{8309364148800} r + 1 \\
& \Delta'(r) = r^7(r-1)(-\frac{1}{304}r^{27} - \frac{25197109151333}{398849479142400}r^{26} - \\
& \frac{79418092024874684869}{13066308936705024000}r^{25} - \frac{15143937856292402262196129}{387350728428620436480000}r^{24} - \\
& \frac{2366973910210561053038186471}{12494385096193580799098800}r^{23} - \frac{8455314295207479062300968873111}{114531863381774490658406400000}r^{22} - \\
& \frac{1249438509611155001115787513}{991524478799860112838020328209849}r^{21} - \frac{5521164844468759159410730585869037}{8246294163487763327405260800000}r^{20} - \\
& \frac{4123147081743881663702630400000}{985364585564805190812437620862539}r^{19} - \frac{111731529120083126099350945280644519}{3298517665395105330962104320000}r^{18} - \\
& \frac{61083660470279728351150080000}{205460937088057311653205176835961321}r^{17} - \frac{1099505884650351103207014400000}{110734493670303732761555001115787513}r^{16} - \\
& \frac{3298517665395105330962104320000}{158032724138819990637134255263110231}r^{15} - \frac{1099505884650351103207014400000}{19980272099587550846028885619407237}r^{14} - \\
& \frac{1099505884650351103207014400000}{224538609583176412587468836353029011}r^{13} - \frac{1099505884650351103207014400000}{24094663993232446388630691852040643}r^{12} - \\
& \frac{1099505884650351103207014400000}{15076783647126646217505642437799077}r^{11} - \frac{1178042023355394761057894400000}{53451052002645000374177015848862851}r^{10} - \\
& \frac{8246294163487763327405260800000}{34157793854758098280948500692837}r^9 - \frac{3665019628216783701069004800000}{6134982182129497498119956432252281}r^8 - \\
& \frac{3298517665395105330962104320000}{5639056379567408901354673628901377}r^7 - \frac{942433618684315808846315520000}{188407735315407315236389143533570237}r^6 - \\
& \frac{157072269780719301474385920000}{218101089181656220622956529171233}r^5 - \frac{1099505884650351103207014400000}{85136118048946532310061747931273}r^4 - \\
& \frac{314144539561438602948771840000}{132994911304258723701851574251}r^3 - \frac{3665019628216783701069004800000}{7962176889165735281009056253}r^2 - \\
& \frac{2157586123361528866406400000}{562493367795228941554181}r - \frac{6544677907529970894766080000}{1060703020501283} \\
& 354149237420452970496000r - \frac{10303182674104320}{8309364148800}) \\
& \Delta''(r) = r^{37} + \frac{142590263789341}{8309364148800}r^{36} + \frac{690448144030236791}{4697039160253440}r^{35} + \\
& \frac{324617284268784317447995081}{387350728428620436480000}r^{34} + \frac{64035135072994828494392138177}{178956036534022641653760000}r^{33} + \\
& \frac{10927345392515915835176820297601}{894780182670113208268800000}r^{32} + \frac{306957477135913987153449321197}{8837335137482599587840000}r^{31} + \\
& \frac{3484547676090740918893922667907}{41099509743209894707200000}r^{30} + \frac{46792604023787574552501267885526031}{257696692608992603981414400000}r^{29} + \\
& \frac{5114092033360339711269496525056973}{147255252919424345132236800000}r^{28} + \frac{82720849919587634913418754596993721}{1374382360581293887900876800000}r^{27} + \\
& \frac{7889974227256354217659306239108441937}{8246294163487763327405260800000}r^{26} + \frac{11624280269542628969132052974659677181}{8246294163487763327405260800000}r^{25} + \\
& \frac{190566613632525673986701170263208391}{98170168612949563421491200000}r^{24} + \frac{78568005593981519178754523078759401}{3123596274083951997747200000}r^{23} + \\
& \frac{1058860227495618987685429305456054977}{343595590145323471975219200000}r^{22} + \frac{7383623302044652471116888965793050837}{2061573540871940831851315200000}r^{21} + \\
& \frac{1716965580898187107499130859630048009}{34278818580615368782242631553834901977}r^{19} + \frac{824629416348776332740526080000}{434015482288829648810803200000}r^{18} + \\
& \frac{34278818580615368782242631553834901977}{1716965580898187107499130859630048009}r^{17} + \frac{824629416348776332740526080000}{434015482288829648810803200000}r^{16} + \\
& \frac{7383623302044652471116888965793050837}{2061573540871940831851315200000}r^{15} + \frac{1058860227495618987685429305456054977}{343595590145323471975219200000}r^{14} + \frac{7383623302044652471116888965793050837}{98170168612949563421491200000}r^{13} + \\
& \frac{11624280269542628969132052974659677181}{7889974227256354217659306239108441937}r^{12} + \frac{824629416348776332740526080000}{824629416348776332740526080000}r^{11} + \\
& \frac{827208499195876349134187545906993721}{511409203360339711269496525056973}r^{10} + \frac{14725525291942434513223680000}{824629416348776332740526080000}r^9 + \\
& \frac{46792604023787374552501267885526031}{257696692608992603981414400000}r^8 + \frac{34845476760990740918893922667907}{41099509743209894707200000}r^7 + \\
& \frac{306957477135913987153449321197}{8837335137482599587840000}r^6 + \frac{10927345392515915835176820297601}{894780182670113208268800000}r^5 + \\
& \frac{640351350752994828494392138177}{324617284268784317447995081}r^4 + \frac{824629416348776332740526080000}{8309364148800}r^3 + \\
& \frac{178956036534022641653760000}{690448144030236791}r^2 + \frac{142590263789341}{8309364148800}r + 1
\end{aligned}$$

Graph ℓ_{10}

$$\begin{aligned}
\Phi'(r) = & r^{49} + \frac{63998337467225103992090545275949}{2453784351049966935520268248500} r^{48} + \\
& \frac{1467791915119732826876236247120465601078713}{4347173063939489764811377306367332725000} r^{47} + \\
& \frac{35863545786298851175250332766194774847587066497001}{12401832675459773375542137748470045164516250000} r^{46} + \\
& \frac{10107225020718561540118243112729380257297990160772275379}{548483451904883937306726584063836217445895672500000} r^{45} + \\
& \frac{17397736112593212118849985482353558760254598400369231894071}{186745556243805721511575956002687093082769240875000000} r^{44} + \\
& \frac{1584820175953684739314764508568609751473509134206333820165933161}{407298147697482280331818969259976807090284812796875000000} r^{43} + \\
& \frac{517274463035147513860432834351215563141952618105299637199565311977}{3747142958810083704990527345171917866252306202777312500000000} r^{42} + \\
& \frac{4952120295981354300300871711979186627645861149}{116654476849271816394836680245746811467802058891725281250000000} r^{41} + \\
& \frac{232819629505635204261122698697497213530179530184438758651042497936165479}{20262186184080608407386744274028037588903678512723178515625000000} r^{40} + \\
& \frac{14070516194229359931408566837646261771234457962573176050687488215725213}{5078812100017226460714996879269928341394111617092968750000000} r^{39} + \\
& \frac{70477610903605497182923534672076616789810509486535754147964424687649474571}{11732055951029389312425164277184135344686203978354531757812500000000} r^{38} + \\
& \frac{56092389787980207748238977346120935042736323202881495578421471399410965213}{47514826601669026715321915322595748145979126112335836191406250000000} r^{37} + \\
& \frac{50266749485106143928653677124964075300401734211654584203734622109856518280909}{2375741330083451335766095766127978749729895630561792689057031250000000} r^{36} + \\
& \frac{26429824010345335688749171370572651127697436882617726500323235117106612145203}{76023722562670442744510504516153197033566017797373657906250000000} r^{35} + \\
& \frac{20823387297836818281526008435918371919883630252711427765368887472917082446989053}{3959568883472418892943492943549645678831593842694654468261718750000000} r^{34} + \\
& \frac{21824947647218174895349817853365257369680047412113598696562977826835140353}{29696766626043141697076197066223425912369538202099085119628906250000000} r^{33} + \\
& \frac{120736166827392932701560441487497944105428801132787147973960403995706625725384629}{1269092590856544516969068251137706948343459564966235406494140625000000} r^{32} + \\
& \frac{135789940566315840585532565857821740547661945056372353589849669605940440768457227}{11878706650417256678830478830648937036494781528083963404785156250000000} r^{31} + \\
& \frac{126393866501084509152854131320795020467290201523310371883484596474040356624342127}{98989222086810472323587323587411419707898460673663617065429968750000000} r^{30} + \\
& \frac{389376833925859979843728937074950725159562999271918086462520859044296962887753}{2934463105340231392991719078717622785695351168004931671142578125000000} r^{29} + \\
& \frac{1216824486333618529509731068844095677597145314078985319601165771484375000000}{948172625352590731068844095677597145314078985319601165771484375000000} r^{28} + \\
& \frac{34295065886761457556474744874331740488184698908469832117314061325299}{29696766626043141697076197066223425912369538202099085119628906250000000} r^{27} + \\
& \frac{136620889917538222852217823124817295526976539096842805176370201484115198050916799}{14141317440972924617655331941248734567255692295338051672363281250000000} r^{26} + \\
& \frac{10610372870896170772509565755154094753809519630524214452593627351709782825503313}{14141317440972924617655331941248734567255692295338051672363281250000000} r^{25} + \\
& \frac{496044793580204554525678229969923834502352531064764912680884504837714700470547}{918835601053315027756070454103414065322925551367880832672119140625000} r^{24} + \\
& \frac{772359485631887562259954215045523575230361655837890625000000}{21519396105828363548605939910595900428432575230361655837890625000000} r^{23} + \\
& \frac{652516365227985670696129273551680629147392704119960328347885247676692854839209}{296967666260431416970761970766223425912369538202099085119628906250000000} r^{22} + \\
& \frac{366302474006714462094696169744275733530561389031328559133377417403031631339261}{296967666260431416970761970766223425912369538202099085119628906250000000} r^{21} + \\
& \frac{1645494418668165225995421450087917210711608999941997419463709015853368829896609}{26049795286002755874762843049668721571260485807201674133300781250000000} r^{20} + \\
& \frac{3483355672276308965949818320346901356561788146343938446724446742989813395385516279}{118870665041725667830478830648937036494781528083963404785156250000000} r^{19} + \\
& \frac{363660177593241450554920575127947967457341872160719024002888028025852967255521}{296967666260431416970761970766223425912369538202099085119628906250000000} r^{18} + \\
& \frac{1566098453886886032512195177922507302933744244599563429255680654923560486349}{343712576690314140984683128965176353632178355422592163085937500} r^{17} + \\
& \frac{984998529036907258351936904704912306334259367334393354862485706731390361}{6599281472450314882391549051607613138598973782442411376953125000000} r^{16} + \\
& \frac{76122446716433949660024957577153519418495869834487283774206365930539589}{1795722849647355507003851675079204389492786323217530371093750000000} r^{15} + \\
& \frac{17803318924131769459327982155770314406131540035651123394684892300797027}{1740469838889753375579315845998100585315974810837128906250000000} r^{14} + \\
& \frac{66682395619516846359952872220117109274829807880728490758393042227}{32694089206142112098386011380595437223355235743605468750000000} r^{13} + \\
& \frac{50241672766902471992514270225360386829136967407233164892842561}{155686139076867200468504816098073510587405884493359375000000} r^{12} + \\
& \frac{2030900035716818913101617969376566049956724765897987917111}{53446944490858694730872157429537304821434882125000000} r^{11} + \\
& \frac{2231094028186541795006656736377928879201619060106379}{75358358271022928497217850902161732770498046875000} r^{10} + \\
& \frac{2160930461505967730083659877408854787}{188694313523723272722487699296875000} r^9
\end{aligned}$$

$$\begin{aligned}
\Phi''(r) = r^{49} + & \frac{66452121818275070927610813524449}{2453784351049966935520268248500} r^{48} + \\
& \frac{3171065904103137883917151919165713711668601}{16155146680896107863213416098535762926181985772279} r^{47} + \\
& \frac{8694346127878979529622754612734665450000}{16155146680896107863213416098535762926181985772279} r^{46} + \\
& \frac{49607330701839093502168550993880180658065000000}{2068529647022090441678077299141302609199588004130495071} r^{45} + \\
& \frac{95388426418240684748995927663275863903634030000000}{450435638313535005425039251624357069084344950220101681650037} r^{44} + \\
& \frac{39216566811199201517430950760564289547381540583750000000}{6867963997466308046319209185518123663135600673726493180976212363} r^{43} + \\
& \frac{13625974395673031654511008527897883150008386191917500000000}{269061418914533471263783319921967679903930817801083532938975715087} r^{42} + \\
& \frac{1427483093523448660768454013952468807724850000000000}{10872394332592778242888786215567008404159907683532322461450204898552609} r^{41} + \\
& \frac{1773148048108931609201517539735351534310591295154224275000000000}{38291101140138887359786276914615116290529958340221391656013420168256811577} r^{40} + \\
& \frac{2172106358933441221271858986175805629530474336563924736875000000000}{985149580003546774556438146762453493111554941047572568221654907248284623} r^{39} + \\
& \frac{2172106358933441221271858986175805629530474336563924736875000000000}{26732729318515826831791274995615639753912223549102534868243984792082723} r^{38} + \\
& \frac{25341240854223480914838354838717732344522200593245788596875000000000}{42518374152731139825902735242032976436330396623572748203732400678572174677} r^{37} + \\
& \frac{1900593064066761068612876612903829925839165044493434144765625000000000}{82807264851056126318963209929741089832356566136075420452698337442115035231749} r^{36} + \\
& \frac{1900593064066761068612876612903829925839165044493434144765625000000000}{149042973009542464340631637361274895460296542764845089050815525174899} r^{35} + \\
& \frac{1900593064066761068612876612903829925839165044493434144765625000000000}{415504848816904463883327746577251726998056709651669094404010048507} r^{34} + \\
& \frac{3167655106777935113545794354839716543065275074155723574609375000000000}{22130456707641639004248146630609315027823814070629995136603247025845612921651603} r^{33} + \\
& \frac{1079882422765520515262095260806805185158892298258148549804687500000000}{1784422236438075188537138900658095059296529954702208506947548731323074538577597981} r^{32} + \\
& \frac{59393532520862833941523941532446851824739076404981702392578125000000000}{328715101921284821780798474559177366372276860411583588494571887934733431113199393} r^{31} + \\
& \frac{79191377669448377858869858870992913576631876853893089365234375000000000}{1289183016088704231293055611652739759836943783125311241033891470144462896563509} r^{30} + \\
& \frac{237574133008345133576609576612978740729895630561679268095703125000000000}{1143364706849144471368732701620706675895368660811433194915842968849736588740046217} r^{29} + \\
& \frac{1696958092916759541186398299498481480706830754405662096835937500000000}{1894223361894024164709180344193508276149281595391591986658211519315337547323846207} r^{28} + \\
& \frac{237574133008345133576609576612978740729895630561679268095703125000000000}{21428097029880732183111243558229670656891082066760972501955864501432138378896531} r^{27} + \\
& \frac{237574133008345133576609576612978740729895630561679268095703125000000000}{801022019708817904455746198578617530054038040854412364759411591253792343583646439} r^{26} + \\
& \frac{819221148304638391643481298665443935513642433161354072266525000000000}{60438310926250885541215047733673129681002510108096187925439945057336154334932897427} r^{25} + \\
& \frac{59393532520862833941523941532446851824739076404981702392578125000000000}{60438310926250885541215047733673129681002510108096187925439945057336154334932897427} r^{24} + \\
& \frac{59393532520862833941523941532446851824739076404981702392578125000000000}{801022019708817904455746198578617530054038040854412364759411591253792343583646439} r^{23} + \\
& \frac{81922114830463839164348129865443935513642433161354072266525000000000}{21428097029880732183111243558229670656891082066760972501955864501432138378896531} r^{22} + \\
& \frac{237574133008345133576609576612978740729895630561679268095703125000000000}{1894223361894024164709180344193508276149281595391591986658211519315337547323846207} r^{21} + \\
& \frac{237574133008345133576609576612978740729895630561679268095703125000000000}{1143364706849144471368732701620706675895368660811433194915842968849736588740046217} r^{20} + \\
& \frac{1696958092916759541186398299498481480706830754405662096835937500000000}{1289183016086188704231293055611652739759836943783125311241033891470144462896563509} r^{19} + \\
& \frac{237574133008345133576609576612978740729895630561679268095703125000000000}{328715101921284821780798474559177366372276860411583588494571887934733431113199393} r^{18} + \\
& \frac{79191377669448377858869858870992913576631876853893089365234375000000000}{1143364706849144471368732701620706675895368660811433194915842968849736588740046217} r^{17} + \\
& \frac{59393532520862833941523941532446851824739076404981702392578125000000000}{1784422236438075188537138900658095059296529954702208506947548731323074538577597981} r^{17} + \\
& \frac{59393532520862833941523941532446851824739076404981702392578125000000000}{22130456707641639004248146630609315027823814070629995136603247025845612921651603} r^{16} + \\
& \frac{107988242276552051526209526080518513588922982581485498046875000000000}{415504848816904463883327767743277601617985477251726998056709651669094404010048507} r^{15} + \\
& \frac{3167655106777935113545794354839716543065275074155723574609375000000000}{1490429730095424643406351637316546813631274895460296542764845089050815525174899} r^{14} + \\
& \frac{1900593064066761068612876612903829925839165044493434144765625000000000}{82807264851056126318963209929741089832356566136075420452698337442115035231749} r^{13} + \\
& \frac{1900593064066761068612876612903829925839165044493434144765625000000000}{42518374152731113983259020275420036623572748073723400678572174677} r^{12} + \\
& \frac{1900593064066761068612876612903829925839165044493434144765625000000000}{26732729318515826831791274995615639753912223549102534868243984792082723} r^{11} + \\
& \frac{25341240854223480914838354838717732344522200593245788596875000000000}{985149580003546774556438146762453493111554941047572568221654907248284623} r^{10} + \\
& \frac{2172106358933441221271858986175805629530474336563924736875000000000}{3829110114013888735978627691461516290529958340221391656013420168256811577} r^9 + \\
& \frac{2172106358933441221271858986175805629530474336563924736875000000000}{10872394332592777284288878621556700840415990768352322461450204898552609} r^8 + \\
& \frac{1773148048108931609201517539735351534310591295154224275000000000}{269061418914533471263783319921967679903930817801083532938975715087} r^7 + \\
& \frac{14274830319276509352344866076845041395246880772485000000000}{6867963997466308046319209185518123663135600673726493180976212363} r^6 + \\
& \frac{136259743956730316545110085278978831500083861919175000000000}{450435638313535005425039251624357069084344950220101681650037} r^5 + \\
& \frac{3921656681119920151743095076054289547381540583750000000}{2068529647022090441678077299141302609199588004130495071} r^4 + \\
& \frac{95388426418240684748995927663275863903634030000000}{16155146680896107863213416098535762926181985772279} r^3 + \\
& \frac{496073307018390935021685509938801806580650000000}{3171065904103137883917151919165713711668601} r^2 + \\
& \frac{8694346127878979529622754612734665450000}{24537843510499669355520268248500} r +
\end{aligned}$$

$$\begin{aligned}
\Delta'(r) = & (r-1)r^9(-\frac{81}{26800}r^{45} - \\
& \frac{563319538758565590920518332973}{6524782699847965260642688600000}r^{44} - \\
& \frac{185118512906802958216749583829138613138971}{150272649123834214092245141454673230000000}r^{43} - \\
& \frac{11292851072467750513499229152350823090599713979537}{964586985869093484764388491547670179462375000000}r^{42} - \\
& \frac{2795138164594878537988787463235668294504668152854207}{33521785350500179520029738666565656731811250000000}r^{41} - \\
& \frac{608279423492031788683211998358870186907289615783102254391}{12810745158325072495694110581784334585477969924025000000000}r^{40} - \\
& \frac{8562912202100990311905987439041329717463210575569086154366093523}{38014493093249194375000000000}r^{39} - \\
& \frac{4462165570512313607734766214843260751907658760237116789155653}{48712858464531088164875584872349322612799806361050625000000000}r^{38} - \\
& \frac{80492686432889156295605195823804626469146709501499514533353144038439997}{2468302680606183205990748847927051851739175382459005382812500000000}r^{37} - \\
& \frac{215746710904829379195187318479384875569690496310367800179931386703}{208856380666677040506909517901519772072379169773004554687500000000}r^{36} - \\
& \frac{2394159327258725649398734336560208580771365396772351115918617324986847}{812219258148188499860203680728132446939814121578390661562500000000}r^{35} - \\
& \frac{28641097615802981958553267946979468109543713475889363519184564264830177497}{3741324929265277694198358521728935548015059930973113085937500000000}r^{34} - \\
& \frac{1823892724320361051151326792463963643515150426030137569700252876097945396887}{1000312138982505825585724533107278908336402654996544286717875000000000}r^{33} - \\
& \frac{70499700652416486993348713309211562159860420872071990636420557270453364200547}{1759808392654408396833774641577620301702930596753179763671875000000000}r^{32} - \\
& \frac{19373207286072881761520568818558588851393956298385872467385979712781}{23575413300834513357660957661297874072989563056167926809570312500000000}r^{31} - \\
& \frac{183229707773937520910155652073606115259697013470625694328906663299547816303896081}{118787066504172566788304788306489370364978152808396340478515625000000000}r^{30} - \\
& \frac{80690365377769302841410373659439059544672078289902985512877385073728956242240459}{29696766626043141697071970766223425912369538202990985119628906250000000}r^{29} - \\
& \frac{2651185883194499040887504690774936941328600647969758044518695964220145865382569}{593935332520862833941523941532446851824739076404198170239257812500000000}r^{28} - \\
& \frac{208357604885427163154003094265059665124071798476776960396417115314565417433}{30433110962332251692912050596831398028364839680590820312500000000}r^{27} - \\
& \frac{1942648826311685890114319916712181216667262683895205966558507624928619658101}{197978441173620944647174647174828394157969213473272341308593750000000}r^{26} - \\
& \frac{6174768978107861419038912615027599943737329385627295727458353708683921405584637}{4695140968544370228786750525948196457112561868807890673828125000000000}r^{25} - \\
& \frac{1959429974773129382885914249383125905939334996397697276431408852173926975516152184711}{118787066504172566788304788306489370364978152808396340478515625000000000}r^{24} - \\
& \frac{2001247114991090534571241484771424435709517984224909784074027410747}{103293101307976145033085115708603220564763611137735948242187500000000}r^{23} - \\
& \frac{1101215958042911685380951714390617129561847691010495425598144531250000000}{5164655065398807251665425578543016102823818055688679741210937500000000}r^{22} - \\
& \frac{326615826789904548993876020347565973369126840229159564065219595833069862596943361}{1484838331302157084853809853831117129561847691010495425598144531250000000}r^{21} - \\
& \frac{28950987185871414926281730160961075903162648944625754003203015534612546931}{136067659225856319345137214554970841884247211089163383789062500000000}r^{20} - \\
& \frac{176309092159642651828702224312993175265953772107682256656404896589851483251201}{9137466654167120522177291408191490028072908867756894926757812500000000}r^{19} - \\
& \frac{541053520848181977923312526312164159051453433388927933669020289977649717366487}{32996407362270157441195774529580380656929948689122120568847656250000000}r^{18} - \\
& \frac{15496496874833837445498705180646917896730804238877170090170310032316093437520631}{11878706650417256678830478830648937036497815280839634047851562500000000}r^{17} - \\
& \frac{1135420222193602957320608891428099418884365703673049006806329037681831956344373}{117031592614948341663354712379205619359091776165907724609375000000000}r^{16} - \\
& \frac{11330668168315454557188211564388453722696718505272870803240987136670851550989}{1683704929826213823801900512606394097873427064228662109375000000000}r^{15} - \\
& \frac{845783523185558343180684251492379416059513047232748269493859485784343700267}{194828713308467388532564848788731130662535370314645947265625000000000}r^{14} - \\
& \frac{5136997041921364612112546442178345709278066935905959887612494862149982516339931}{19797844117362094464717464717748228394157969213473272341308593750000000}r^{13} - \\
& \frac{217833415291497478774331715205998246465590849994367955140829072881017947763137}{1522911109027853420362881901365248338012151477959482487792968757300000000}r^{12} - \\
& \frac{396611250527760547918131357972016980601794540953794150895806492299908416797}{54841672863215913150068274729867822552852323783193139648437500000000}r^{11} - \\
& \frac{1099102683811529195240817760036078549127470602338328818688702513211800499}{32996407362270157441195774529580380656929948689122120568847656250000000}r^{10} - \\
& \frac{54891046981614005762550314166628632335458897980274085132835191057226547333}{395956888347241889294349235496456783193832469465446826171875000000000}r^9 - \\
& \frac{61310683215913150068274729867822552852323783193139648437500000000}{11878706650417256678830478830648937036497815280839634047851562500000000}r^8 - \\
& \frac{2689414305873757566525592643024364570485198203754824699833483392541589960819}{158382755338896575571773917741985827153263753708617873046875000000000}r^7 - \\
& \frac{16492262328368239754680273310812198254876823173073900932151067207404659961}{3393916185833501908237279665899696296141366150881132401367187500000000}r^6 - \\
& \frac{206252898674636190464249334702901618990003672145157753323380738467272477}{174046983888975337557579315845998100585315974810837128906250000000}r^5 - \\
& \frac{352291059682303397502433427535140117512763041819685007703823551579}{1471234014276395044427370512126794675050985608462246093750000000}r^4 - \\
& \frac{29962903292647976025325503049075929992044225870272449515704223}{7784306953843360023425240804903675529370294224667968750000000}r^3 - \\
& \frac{239277682879825336161377672215173406914951652136521829783}{5184353615132933888945992706651185676791836328125000000}r^2 - \\
& \frac{94197947838778866062152231362770216596312255859375}{273987326268735002858812178111979787}r - \\
& 1886943135237232727224847699296875000
\end{aligned}$$

$$\begin{aligned}
\Delta''(r) = & r^{57} + \frac{66452121818275070927610813524449}{2453784351049966935520268248500} r^{56} + \\
& \frac{3179760250231016863446774673778448377118601}{16289490694520104637404694861769225591462519982279} r^{55} + \\
& \frac{8694346127878979529622754612734665450000}{48378563499458279070496997046791674658021454156922194833} r^{54} + \\
& \frac{49607330701839093502168550993880180658065000000}{2193933807619535749226906336255344869783582690000000} r^{53} + \\
& \frac{231656564107404127657533499876345428450010894244108883079531}{1960828340559960075871547538028214477369077029187500000} r^{52} + \\
& \frac{71684311607205685505629840926485056517907420131597702535267113}{13625974395673031654511008527897883150008386191917500000000} r^{51} + \\
& \frac{285926016781552491757251758712965627095091610902054659627165571887}{14274830319276509352344866013952468807724850000000000} r^{50} + \\
& \frac{11805222279537344870098094733640434340820666060934047270481119207967299}{1773148048108931609201517539735351534310591295154224275000000000} r^{49} + \\
& \frac{294081709734604509298806812052828737227843923112119641403310046791028651}{149800438547133877329093723184538319227796374734923618875000000000} r^{48} + \\
& \frac{18829392186702609980137135872634107599504106048177001370983}{362017726488906870211976497695967604921745722760654122812500000000} r^{47} + \\
& \frac{47561407068113171420696418508451533053175046368911395678068968300303173325997}{380118612813522137225753225807659851678330088986828953125000000000} r^{46} + \\
& \frac{524037357309638139993594284647384667702228606494496816682135156818346707335427}{19005306406676106861278661290382992583916504493434144765625000000000} r^{45} + \\
& \frac{8459313447387326074946740580599724377967091359021440657895512613663035609}{15084071937037786258832354070665316871739405115027255117187500000000} r^{44} + \\
& \frac{28777512463063488956648718087102988792698775953323161327217307672552413629167}{271513294866680152658982373271975703691309292070490592109375000000000} r^{43} + \\
& \frac{257875730434961337682776258615935312520159903506447727051475200597178416409}{137724135077301526711078015427813762741968481485031459765625000000000} r^{42} + \\
& \frac{492369024007770206158732745957266597900056372641367109988420049606172193809987419}{15838275533889675751773971498582715326375370778617873046875000000000} r^{41} + \\
& \frac{82725473941191597120414616524708494240159395260501186283522913598100754467252691}{169695804911675095411863983299498418070683075440268359375000000000} r^{40} + \\
& \frac{861621055408051894533099499459364853363012529112111429131028867463619051637282857}{1187870665041725667883047883064893703649478152808396340478515625000000000} r^{39} + \\
& \frac{2443151562075668373112121456670035630778212944866802042856090000353452413775807833}{237574133008345133576609576612978740729895630561679268095703125000000000} r^{38} + \\
& \frac{5521962711456028760426891066551076472363379775969429960353154893961457922388134417}{395956888347241889294349294354964567883159384269465464862617187500000000} r^{37} + \\
& \frac{215615049511679197508324870277576682026533654142781306830097403451271092619370889}{1187870665041725667883047883064893703649478152808396340478515625000000000} r^{36} + \\
& \frac{180094645405691272853633604334198126975439052098418469175609769133977152496452261}{79191377669448377858869588709929135766318768538930889365234375000000000} r^{35} + \\
& \frac{65317677663253357151894511940209678389193319121349043905904031459876355124802259}{237574133008345133576609576612978740729895630561679268095703125000000000} r^{34} + \\
& \frac{6361723402465013906139013079761450330385115708603220564763611137359482421875000000000}{1979784441736209446471746471774822839415796921347327234130859375000000000} r^{33} + \\
& \frac{332218137183117318606269693439063144199401878066104511021752322523938976696259767}{91374666541671205221772914081914900280729088677568949267578125000000000} r^{32} + \\
& \frac{4117461692411435385433658921230255753386348979644534206373486498604632172945064269}{1032931013079761450330385115708603220564763611137359482421875000000000} r^{31} + \\
& \frac{10066712375173857530179267712688226692532522009276644231277321324831547378171258549}{237574133008345133576609576612978740729895630561679268095703125000000000} r^{30} + \\
& \frac{5823928141793754818105611918824670762409658757859402832597412456373577529537229}{1333188176253339694593768667861833561896159542994833154296875000000000} r^{29} + \\
& \frac{5823928141793754818105611918824670762409658757859402832597412456373577529537229}{1333188176253339694593768667861833561896159542994833154296875000000000} r^{28} + \\
& \frac{10066712375173857530179267712688226692532522009276644231277321324831547378171258549}{237574133008345133576609576612978740729895630561679268095703125000000000} r^{27} + \\
& \frac{4117461692411435385433658921230255753386348979644534206373486498604632172945064269}{1032931013079761450330385115708603220564763611137359482421875000000000} r^{26} + \\
& \frac{332218137183117318606269693439063144199401878066104511021752322523938976696259767}{91374666541671205221772914081914900280729088677568949267578125000000000} r^{25} + \\
& \frac{6361723402465013906139013079761450330385115708603220564763611137359482421875000000000}{1979784441736209446471746471774822839415796921347327234130859375000000000} r^{24} + \\
& \frac{65317677663253357151894511940209678389193319121349043905904031459876355124802259}{237574133008345133576609576612978740729895630561679268095703125000000000} r^{23} + \\
& \frac{180094645405691272853633604334198126975439052098418469175609769133977152496452261}{79191377669448377858869588709929135766318768538930889365234375000000000} r^{22} + \\
& \frac{2156156495116791975083248702775766820265336541427813068300970403451271092619370889}{1187870665041725667883047883064893703649478152808396340478515625000000000} r^{21} + \\
& \frac{5521962711456028760426891066551076472363379775969429960353154893961457922388134417}{3959568883472418892943492943549645678831593842694654648626171875000000000} r^{20} + \\
& \frac{237574133008345133576609576612978740729895630561679268095703125000000000}{24431516520756683731121456670035630778212944866802042856090000353452413775807833} r^{19} + \\
& \frac{8616210554080518945933099499459364853363012529112111429131028867463619051637282857}{1187870665041725667883047883064893703649478152808396340478515625000000000} r^{18} + \\
& \frac{8272547394119159712041616524708494240159395260510186283522913598100754467252691}{169695804911675095411863983299498418070683075440268359375000000000} r^{17} + \\
& \frac{4923690240077702061587287459572656979000563726413671098842049606172193809987419}{15838275533889675571773971498582715326375370778617873046875000000000} r^{16} + \\
& \frac{2578756730434961337682727762586159353112520159903506447727051475200597178416409}{137724135077301526711078015427813762741968481485031459765625000000000} r^{15} + \\
& \frac{28777512463063488956648718087102988792698775953323161327271370672552413629167}{2715132948666801526589823732719757036913092920704905921093750000000000} r^{14} + \\
& \frac{8459313447387326074946974058059972437796587091359021440657895512613663035609}{150840719370377862588323540706653168717394051150272551171875000000000} r^{13} + \\
& \frac{524037357309638139993594284647384667702228606494496816682135156818346707335427}{19005306406676106861287661290382992583916504493434144765625000000000} r^{12} + \\
& \frac{475614070681131714206964185084515330531750463689113956780689683003017332597}{380118612813352213722575322580765985167833008898686828953125000000000} r^{11} + \\
& \frac{18829392186780260998012126575519180137135872634107599504106048177001370983}{3620177264889068702119764976959676049217457227606541228125000000000} r^{10} + \\
& \frac{294081709734604509298806812052828737227843923112119641403310046791028651}{1498004385471338773290937231845383192779637473492361887500000000000} r^9 +
\end{aligned}$$

$$\begin{aligned}
& \frac{11805222279537344870098094733640434340820666060934047270481119207967299}{1773148048108931609201517539735351534310591295154224275000000000} r^8 + \\
& \frac{285926016781552491757251758712965627095091610902054659627165571887}{7168431160720568553056298409926485056517907420131597702535267113} r^7 + \\
& \frac{142748303192765093523448660768454013952468807724850000000000}{31656564107404127657533499876345428450010894244108883079531} r^6 + \\
& \frac{13625974395673031654511008527897883150008386191917500000000}{48378563499458279070496997046791674658021454156922194833} r^5 + \\
& \frac{1960828340559960075871547538028214477369077029187500000}{162894906945201046374046948661769225591462519982279} r^4 + \\
& \frac{219393380761953574922690633625534486978358269000000}{3179760250231016863446774673778448377118601} r^3 + \\
& \frac{49607330701839093502168550993880180658065000000}{8694346127878979529622754612734665450000} r^2 + \\
& \frac{66452121818275070927610813524449}{2453784351049966935520268248500} r + 1
\end{aligned}$$

¹ GEODYNAPP - ECSING GROUP, SPAIN.

² DEPARTAMENTO DE MATEMÁTICAS, UNIVERSIDADE DE SANTIAGO DE COMPOSTELA, E-15782, SANTIAGO DE COMPOSTELA, SPAIN.

E-mail address: fernando.alcalde@usc.es

¹ GEODYNAPP - ECSING GROUP

³ DEPARTAMENTO DE DIDÁCTICAS APLICADAS, FACULTADE DE FORMACIÓN DO PROFESORADO, UNIVERSIDADE DE SANTIAGO DE COMPOSTELA, AVDA. RAMÓN FERREIRO 10, E-27002 LUGO, SPAIN

E-mail address: pablo.gonzalez.sequeiros@usc.es

¹ GEODYNAPP - ECSING GROUP

⁴ CENTRO UNIVERSITARIO DE LA DEFENSA, ACADEMIA GENERAL MILITAR, CTRA. HUESCA s/n. E-50090 ZARAGOZA, SPAIN

⁵ INSTITUTO UNIVERSITARIO DE MATEMÁTICAS Y APLICACIONES, UNIVERSIDAD DE ZARAGOZA, SPAIN

E-mail address: alvaro.lozano@unizar.es